EUROPEAN SPALLATION SOURCE LATTICE DESIGN STATUS

Y. Inntjore Levinsen*, H. Danared, M. Eshraqi,
R. Miyamoto, A. Ponton, R. de Prisco, E. Sargsyan, ESS, Lund, Sweden
H. Dølrath Thomsen, S. Pape-Møller, ISA, Aarhus Uni., Denmark

Abstract

The accelerator of the European Spallation Source (ESS) will deliver 62.5 mA proton beam of 2.0 GeV onto the target, offering an unprecedented beam power of 5 MW. Since the technical design report (TDR) was published in 2013, work has continued to further optimise the accelerator design. We report on the advancements in lattice design optimisations after the TDR to improve performance and flexibility, and reduce cost of the ESS accelerator.

INTRODUCTION

The ESS project is an ambitious project, which aims to provide a world leading 5 MW spallation neutron source, planned to be commissioned in 2019 [1]. The ESS is constructed in Lund, Sweden, in a collaboration between 17 partner countries. The neutrons are produced by shooting a high power proton beam onto a spallation target. The current accelerator design is assuming operation at 14 Hz, with 2.86 ms long pulses, corresponding to a duty cycle of 4 %. The accelerator can accelerate the beam up to 2 GeV, and a beam current of 62.5 mA is thus needed to reach the 5 MW requirement. The overall layout is shown in Fig. 1.

Since the TDR was published in 2013 [2], the beam energy has been reduced from 2.5 GeV to meet the budget requirements. Correspondingly the beam energy increased from 50 mA to 62.5 mA in order to keep the beam power constant. This was discussed last year in [3]. The high level parameters described within this reference remain unchanged this year.

The accelerator design is currently mainly limited by the amount of power that can be fed to the cavities (energy), beam loss limits (intensity), and space charge effects at low energy.

There has been ongoing work to further optimise and finalise the design of the lattice optics in the last year, and various error studies have been performed to better understand the limitations of the lattice and providing valuable input for the design constraints. The lattice and optics presented here will in the future be referenced to as the "2014 Baseline".

FRONT END

The front end of the ESS linac will accelerate the high intensity beam from the 75 keV ion source and up to 90 MeV at the exit of the last DTL tank, before the beam is injected into the superconducting part of the linac. With a high power superconducting linac, it is important to provide a high quality beam to the superconducting section so as to minimise the losses (machine protection). In addition, it is important to generally keep the losses low, to reduce activation and keep a good machine reliability.

* yngve.levinsen@esss.se

Ion Source, LEBT, and RFQ

The proton beam is generated with a Microwave Discharge Ion Source (MDIS), delivering a 75 keV beam energy and more than 70 mA proton beam current to the low energy beam transport (LEBT) [4]. The LEBT is a 2.4 m long section matching the beam to the RFQ using two solenoids. In between the solenoids a chopper is installed to remove the transient of the beam pulse.

The four-vane RFQ acclerates and bunches the continuous pulse from the source into bunches at 352.21 MHz. The output beam energy of the RFQ is 3.62 MeV. The RFQ has a relatively long bunching section to allow for a higher transmission.

In Fig. 2, we show the transmission through the LEBT+RFQ for different strengths of the two solenoids in the LEBT lattice. The optimal setting found in this simulation is to have the two solenoids at 0.238 T and 0.244 T, providing a transmission of 97.8%. The working point is shown by the large dot in the figure.

MEBT and DTL

Between the RFQ and the start of the drift tubes, there is a section of 3.6 m called the Medium Energy Beam Transport (MEBT). Recent advancements in the MEBT layout was described in [5, 6]. The purpose of this section is to match the beam coming out of the RFQ to the drift tube linac, and to measure the beam properties with various beam diagnostics. The MEBT has 11 quadrupoles for the focusing of the beam, with one BPM per quadrupole. Three scrapers will be installed to clean the transverse halo, which will reduce the losses in the DTL and superconducting part of the linac [7].

A fast chopper is installed in the MEBT, which main purpose is to chop off the bad quality bunches at the beginning and end of the pulse which could not be removed by the LEBT chopper due to the space charge compensation recovery time. Both the LEBT and the MEBT choppers have a secondary purpose of providing an additional level of beam protection. The MEBT chopper is the last location where the beam can be dumped before the superconducting section.

The last accelerating section of the warm linac is the drift tube linac (DTL). The DTL consists of 5 tanks which brings the beam energy from 3.6 MeV to 90 MeV. The DTL has undergone a design optimisation since the TDR was published in 2013. One tank was added, and the output beam energy thus increased from the original 77.5 MeV to 90 MeV [8].

The FODO lattice is realised using permanent magnet quadrupoles (PMQ) in every second drift tube. There are also three horizontal, three vertical steerers, and three BPMs in each tank. The optimised locations of the steerers and BPMs are currently being studied [9].

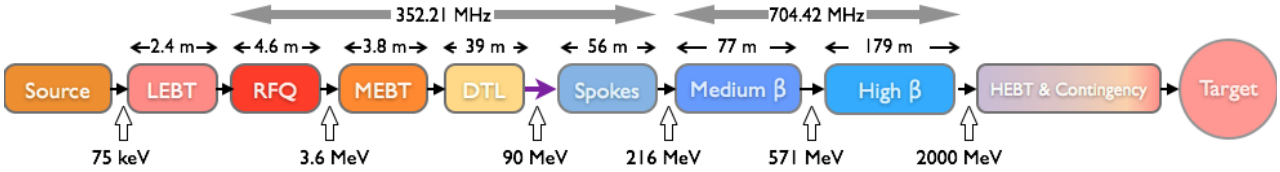

Figure 1: The overall layout of the different sections of the ESS linac. The front end including the spoke cavities run at 352.2 MHz, while the elliptical cavities run at twice that frequency. The beam energy at each intersection is given below the intersections.

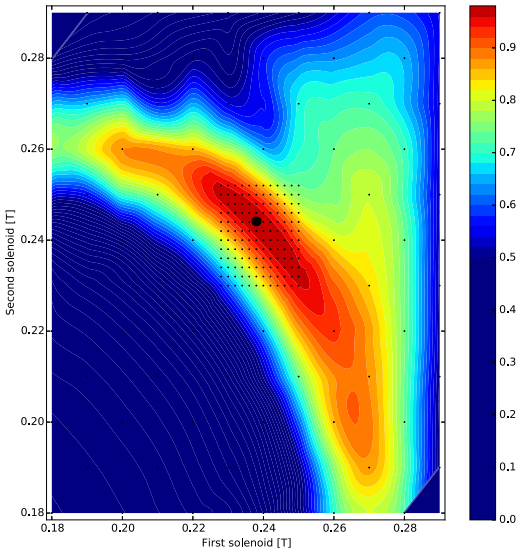

Figure 2: Transmission through the RFQ as a function of the LEBT solenoid strengths. Only accelerated particles are counted. The color bar shows the transmission, where anything dark blue is less than 50%, while 100% is dark red. The small dots show all simulated data points, while the larger dot show the optimal setting found. The color map shows a cubic interpolation between the individual simulated values.

In the past the drift tubes have been represented in a parametrised way. The effects of representing the DTL with field maps instead is discussed in more detail in [10].

SUPERCONDUCTING LINAC

Exiting the DTL at 90 MeV, the acceleration up to 2 GeV is done in three superconducting sections. The first part of the superconducting linac are spoke cavities, accelerating the beam up to 216 MeV using 26 double spoke cavities stored in pairs in 13 cryomodules. Between each cryomodule is a spoke warm unit (SWU), containing normal conducting magnets for focusing and correction, and diagnostics.

After the spoke cavities there are two sections of elliptical cavities. First we have 36 medium-β cavities, with a geometric β of 0.67. After that we have 84 high-β cavities, with a geometric β of 0.86. Four cavities are housed in one cryomodule. The medium-β cavities have one more cell, 6 instead of 5 for high-β, which makes the cavities (and hence also cryomodules) almost equal in length. The elliptical warm units (EWU) are functionally identical to the SWUs, but with bigger apertures and longer quadrupoles. The period length is exactly twice that of the spoke section [3, 11].

3D Field Maps

A recent advancement in the accuracy of our simulations, is the availability of the 3D field maps for the superconducting cavities. The 3D field maps allows for higher precision in tracking simulations. The 1D field maps are defined only by the longitudinal field E_z, along the line $(x,y) = (0,0)$. All other electromagnetic field components are then extrapolated in the simulation code. The 3D field maps on the other hand, holds all three components of both magnetic and electric field, on a 3D grid of points. The simulation code then interpolates between the grid points. This results in a vastly increased data size for the field maps.

Major differences in the simulations were not found, but for example the emittance growth was found to be slightly smaller with 3D field maps, as shown in Fig. 3. The 3D field maps will be used by default from now onwards in our studies of the superconducting lattice.

BEAM DELIVERY SYSTEMS

The general requirements and purpose of the Beam Delivery Systems (BDSs) is described in [12]. It consists of the High Energy Beam Transport (HEBT), a 128 m contingency space for potential extension of the elliptical cavity linac, and a vertical achromatic dogleg. Downstream of the HEBT we have the Accelerator to Target (A2T), which is a beam matching and distribution system. In addition, a low-power dumpline is in line of sight with the accelerator, going straight from the beginning of the dogleg. Following the change from a BDS based on non-linear magnets to the present linear raster-based system, multiparticle tracking simulations through the A2T exhibit vastly improved transmission efficiency. Even when including static and dynamic errors the beam is transported through the very large aperture radius ($\gtrsim 20\times\sigma_{\mathrm{RMS}}$) without observable losses [13]. Consequently, the justification for the two full-energy collimator systems has been revisited through hosting a workshop and assembling an internal working group to review similar systems and facilities. It was agreed to continue the collimator design based on

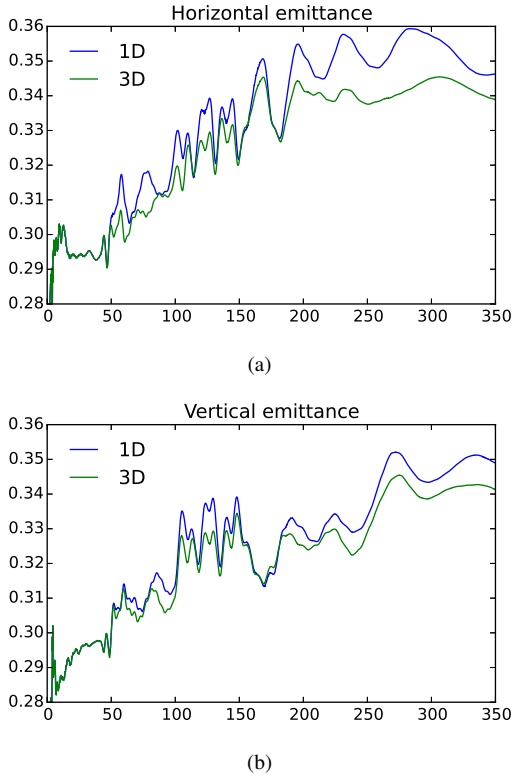

Figure 3: Comparison of emittance growth with 1D and 3D field maps.

existing specifications, but not proceed with the actual construction of the collimator units unless proven necessary [14].

In the A2T, a transverse matching unit consisting of two quadrupole doublets sets a double waist at the so-called crossover (CO) while providing the nominal beamlet size at the target front face, the beam entrance window (BEW). Following requests from the target division, the nominal horizontal (H) and vertical (V) RMS beam size at the target has been reduced by about $\simeq 10\%$ compared to [12]. Combined with changes in the HEBT input beam, this retuning led to a significant vertical higher-order (HO) dispersion at the location of the target, downstream of the linear vertical achromat. The vertical beam position would thus be sensitive to energy jitter or sudden significant energy changes caused by RF problems.

A study of the A2T matching was launched to reduce the dispersive effects in the A2T. As input to a series of TraceWin A2T matching optimisations, the CO double waist requirement was slightly compromised by scanning the requested CO H and V RMS beam size across a grid, while maintaining the nominal beam size at the target. For each optimum quadrupole tuning, the HEBT input energy would be detuned within $|\delta_K| < 100$ MeV to probe the HO dispersion. The exhaustive search provided at least one solution leading to $|\Delta y| < 4$ mm within -100 MeV $< \delta_K < 40$ MeV while meeting the matching requirements.

FAILURE MODES

It is important for the machine protection systems to know what will happen in faulty situations. For example, how much of the beam is lost, and where, in case of a cavity or magnet fault. As a first step in providing such information, we have simulated the losses in cases where the RF of the cavities were completely cut off, and also turned quadrupole magnets completely off [15]. These have been assumed immediate, allowing no correction of the lattice to take place. Loaded Q-value of the cavities or the decay time of the magnets were not taken into account, providing worst case scenario, and in some cases unrealistic scenarios. Based on extrapolation and knowing the rise times of e.g. magnets in case of power failure, one can then estimate for example how fast the machine protection must kick in.

The results show that e.g. if a quadrupole in the superconducting section switches off, about 30-70% of the beam is lost before reaching the target. In the case of 0 power in one DTL tank, there is no transmission to the target, but the location of the major beam losses is depending on which tank is off. For the superconducting linac, there is some transmission to target for cavity failure from approximately the middle of the medium-β cavities onwards, and single cavity failure in the high-β section does not reduce transmission dramatically.

These studies are also relevant for e.g. the discussion of pulsed magnets, and show that in general the machine protection must be sure that all magnets are pulsed before beam permit can be given.

LATTICE REPOSITORY

The different sections of the ESS lattice are often worked on separately, assuming a given set of input parameters. The lattice files for each section would then need to be manually merged for end-to-end studies, and if old input parameters was assumed, rematch would be needed.

This manual procedure is somewhat error prone, and in order to aid the scientists working on the lattice, we have collected the files into a GIT repository. Some of the older files were also committed to the repository so that historical changes can be followed to some extent. A few python scripts are also in place in the repository, automating for example the split&merge of the various lattice parts. The repository can then easily be cloned and developed on by the different parties, without worrying that they will break the stable/official version. This will help tracking changes in the future and understand potential regressions quicker. The repository currently has the 2014 baseline as the stable lattice version.

SUMMARY

The ESS lattice is now in a very mature state, something that is shown by the relatively low amount of changes to the lattice layout itself since last year. A large effort has gone into making a more robust and more detailed lattice description, which allows for a more accurate prediction of the accelerator performance and margins.

REFERENCES

[1] H. Danared, Roland Garoby, and Mats Lindroos. "Status of the ESS Accelerator Construction Project". In: *IPAC 15 Richmond, USA, these proceedings*. THPF080.

[2] *European Spallation Source Technical Design Report*. Tech. rep. 2013.

[3] M. Eshraqi et al. "The ESS Linac". In: *IPAC'14 Dresden, Germany*. 2014.

[4] L. Neri et al. In: *Review of Scientific Instruments* 85.2 (2014). DOI: 10.1063/1.4832135.

[5] Ryoichi Miyamoto et al. "Beam Physics Design of the ESS Medium Energy Beam Transport". In: *IPAC'14 Dresden, Germany*. 2014.

[6] I. Bustinduy et al. "Progress on ESS Medium Energy Beam Transport". In: *LINAC'14, Switzerland*. 2014.

[7] Ryoichi Miyamoto, Mohammad Eshraqi, and Heine D. Thomsen. "An ESS Linac Collimation Study". In: *HB'2014, USA*. 2014.

[8] Renato de Prisco et al. "ESS DTL Status: Redesign and Optimizations". In: *IPAC'14 Dresden, Germany*. 2014.

[9] Ryoichi Miyamoto et al. "A Preliminary Study of Tuning Schemes for the ESS Linac". In: *IPAC 15 Richmond, USA, these proceedings*. MOPJE032.

[10] Renato de Prisco et al. "Effect of the Field Maps on the Beam Dynamics of the ESS DTL". In: *IPAC 15 Richmond, USA, these proceedings*. THPF078.

[11] Mohammad Eshraqi. *Beam Physics Design of the Optimus+ Linac*. Tech. rep. ESS-doc-309-v3. 2013. http://docdb01.esss.lu.se/cgi-bin/public/DocDB/ShowDocument?docid=309

[12] H. D. Thomsen and Søren Pape-Møller. "The ESS High Energy Beam Transport After the 2013 Design Update". In: (2014).

[13] H. D. Thomsen and Søren Pape-Møller. "Performance of the ESS High Energy Beam Transport under Non-nominal Conditions". In: *IPAC'14 Dresden, Germany*. WEPRO074 (2014).

[14] H. D. Thomsen. *A Study of ESS HEBT Collimator Options*. Tech. rep. ESS-doc-360-v4. 2015. http://docdb01.esss.lu.se/cgi-bin/public/DocDB/ShowDocument?docid=360

[15] Mohammad Eshraqi et al. *Preliminary Study of the Possible Failure Modes of the Components of the ESS Linac*. Tech. rep. ESS-0031413. Mar. 2015.